Original Article

Institution of MECHANICAL ENGINEERS

Journal of SYSTEMS AND CONTROL ENGINEERING

Proc IMechE Part I:
J Systems and Control Engineering
2025, Vol. 239(6) 1119–1131

DOI: 10.1177/09596518241309123
journals.sagepub.com/home/pii
Sage

Fault compensation-based adaptive tracking control for nonlinear systems with actuator saturation and multiple sensor faults

Yao-Yao Guo[1,2,3], Yu-Qun Han[1,2,3], Jing-Jing Sun[1,2,3] and Shan-Liang Zhu[1,2,3]

Abstract

An adaptive tracking control scheme based on a multi-dimensional Taylor network(MTN) is proposed for nonlinear systems with multiple sensor faults and actuator saturation. This article utilizes a smooth hyperbolic tangent function to transform the non-smooth actuator saturation model into a smooth linear model, thus addressing the challenges posed by actuator saturation on the system. By applying a third-order absolute value Lyapunov function and incorporating it into the adaptive control design process, the estimation of fault losses and design of compensation coefficients are carried out to eliminate the effects of sensor faults. Experimental results demonstrate that the proposed controller can eliminate the impact of sensor faults and actuator saturation, ensuring that all signals in the closed-loop system remain within bounded ranges. Additionally, it can drive the tracking error to converge to a small region near the origin.

Keywords

Adaptive control, actuator saturation, sensor faults, multi-dimensional Taylor network, nonlinear systems

Date received: 9 July 2024; accepted: 10 November 2024

Introduction

In recent years, control problems of nonlinear systems have been widely studied and significant progress has been made in various fields.[1–3] In particular, the prevalence of sensor faults[4] and actuator saturation[5] in practical engineering places higher demands on nonlinear system control. Unfortunately, many studies tend to overlook these critical issues when discussing nonlinear systems.[6,7] Therefore, It is critical to research on how to improve the control performance and stability of nonlinear systems with multiple sensor faults and actuator saturation.

Recently, a growing attention has been paid on nonlinear systems with actuator saturation due to the fact that the presence of actuator saturation can lead to the instability and performance degradation of control systems. Many control methods have been proposed to deal with the problem of actuator saturation.[5,8,9] Generally, these methods can be divided into two main categories: compensation methods[10–12] and approximation methods.[13–15] Compensation methods primarily identify the presence of actuator saturation constraints and design parameters or compensators to offset their adverse effects on system performance. In contrast, approximation methods introduce a controller to monitor the output of the actuator and adjust the input signal to prevent the occurrence of saturation. Compared to compensation methods, approximation strategies can quickly and efficiently monitor the output state of the actuator in real time, allowing timely responses to actuator saturation.[16–18] By adjusting the input signal, the above methods increase the robustness of the system, enabling stable control performance even under conditions of actuator saturation.[19] However, these

[1]School of Mathematics and Physics, Qingdao University of Science and Technology, Qingdao, China
[2]Qingdao Innovation Center of Artificial Intelligence Ocean Technology, Qingdao University of Science and Technology, Qingdao, China
[3]Shandong Engineering Research Center of Marine Scenarized Application of Artificial Intelligence Technology, Qingdao, China

Corresponding author:
Shan-Liang Zhu, School of Mathematics and Physics, Qingdao University of Science and Technology, 99 Songling Road, Laoshan District, Qingdao 266061, China.
Email: zhushanliang@qust.edu.cn

Table 1. Sensor faults.

Faults kinds	Conditions	Faults names
$x_i^f(t) = \bar{x}_i(t) + b(t)$	$b(t) \neq 0, (\dot{b}(t) = 0)$	Bias fault
$x_i^f(t) = \bar{x}_i(t) + b(t)$	$\lvert b(t)\rvert = \gamma t, 0 < \gamma \ll 1$	Drift fault
$x_i^f(t) = \bar{x}_i(t) + b(t)$	$\lvert b(t)\rvert = \bar{b}, \dot{b} \to 0$	Loss of accuracy fault
$x_i^f(t) = \rho_i(t)\bar{x}_i(t)$	$0 < a_{\min} \leqslant \rho_i(t) \leqslant 1$	Loss of effectiveness fault

methods can be difficult to adapt to nonlinear control systems with faults.

In fact, the presence of faults in a nonlinear system introduces results in system instability and uncertainty in the sign of the measured state. Therefore, it has also been the focus of attention to addressing the problem of faults in nonlinear control systems. Researchers have made strides in enhancing system adaptability in the face of faults.[20–23] Thus far, research on system faults has primarily been categorized into two main areas: actuator faults[24–26] and sensor faults.[27–29] In particular, sensor faults have been initially addressed by different methods such as fault detection techniques and compensation mechanisms.[30,31] These methods have been successfully applied to various nonlinear systems, including uncertain nonlinear systems,[32] uncertain strict-feedback nonlinear systems,[33] and nonlinear discrete-time multi-agent systems.[34] Notably, neural networks and fuzzy logic systems have been utilized in controller design to tackle the unknown nonlinearities inherent in these systems.[22,35,36] Moreover, various network approximation-based adaptive control schemes have been proposed to address a range of issues stemming from sensor or actuator faults.[37–41] However, adaptive control problems for nonlinear systems with both sensor faults and actuator saturation have rarely been studied. There is a great challenge to deal with these issues simultaneously in controller design.

In response to the above challenge, this paper proposes an adaptive tracking control scheme based on multi-dimensional Taylor networks (MTN) to address the issues of multiple sensor faults and actuator saturation in nonlinear systems. That the proposed controller successfully eliminates the effects of sensor faults and actuator saturation, ensuring that all signals within the closed-loop system remain bounded while driving the tracking error into a small region near the origin. Compared with the existing results, the main contributions of this paper are as follows:

(i) This paper introduces a novel adaptive control method based on MTNs to address the tracking control problem in nonlinear systems with multiple sensor faults and actuator saturation. The proposed control method boasts a straightforward structure and minimal computational complexity, leveraging the inherent simplicity of MTNs. Despite the advancements made in utilizing MTNs for nonlinear systems,[42–45] previous efforts have overlooked the critical issue of sensor faults. This paper represents the first attempt to tackle this challenge within the context of MTN-based control.

(ii) In contrast to existing research that solely addresses sensor faults[31,46–48] and focuses on actuator saturation,[49–52] this paper presents a comprehensive analysis of both sensor faults and actuator saturation in nonlinear systems. By integrating various approaches such as saturation model transformation, signal compensation mechanisms, and cubic absolute-value Lyapunov, an innovative and robust control scheme has been developed to address these issues.

Problem description and knowledge preparation

Problem description

In this paper, the following form of nonlinear systems is considered:

$$\begin{cases} \dot{x}_i = x_{i+1} + f_i(\bar{\boldsymbol{x}}_i) + \Delta_i(t) \\ \dot{x}_n = u(v) + f_n(\bar{\boldsymbol{x}}_n) + \Delta_n(t) \\ y = x_1 \end{cases} \tag{1}$$

where $\bar{\boldsymbol{x}}_n = [x_1, \ldots, x_n]^T$ is the state vector of the system with $\bar{\boldsymbol{x}}_i = [x_1, \ldots, x_i]^T \in R^i, i = 1, 2, \ldots, n$, $y \in R$, and $\Delta_i(t)$ represent the measured output, and bounded uncertainties, respectively. $f_i(\bar{\boldsymbol{x}}_i) \in R_i \to R, i = 1, \ldots, n$ is a smooth unknown nonlinear function. u and v represent the output and input of the actuator, and satisfy the following relationship

$$u(v) = sat(v) = \begin{cases} \text{sign}(v)u_m, & |v| \geqslant u_m \\ v, & |v| < u_m \end{cases} \tag{2}$$

where $u_m > 0$ denotes the boundary of u and $sign(\cdot)$ is a symbolic function.

Especially, the following sensor faults are assumed in system

$$x_i^f(t) = \rho_i \bar{x}_i(t), \forall t > T_f \tag{3}$$

where T_f is the time of fault occurrence, ρ_i is a normal constant indicates the loss of effectiveness failure and satisfies $0 < \rho_i \leqslant 1$. A more detailed explanation about the studied faults is presented in Table 1.

Remark 1: In the absence of sensor faults, the nonlinear system (1) has been extensively studied.[1–3,6] Furthermore, in real-world applications, stochastic disturbances are unavoidable. Consequently, system (1) serves as a versatile model for numerous controlled systems.

For the nonlinear system (1) with actuator saturation (2) and multiple sensor faults (3), the goal of this paper is to design an adaptive tracking control scheme, such that

(1) All signals in the closed-loop system are bounded;
(2) The system output y can follow the desired reference signal y_d efficiently.

Actuator saturation pre-processing

Due to the existence of singularities in actuator saturation, it cannot be directly used for controller design. According to Wu et al.,[53] following smooth function $g(v)$ is employed to approximate saturated function $u(v)$

$$g(v) = \frac{2}{\pi}u_m \tanh\left(\frac{\pi v}{2u_m}\right) = \frac{2}{\pi}u_m \frac{e^{\frac{\pi v}{2u_m}} - e^{-\frac{\pi v}{2u_m}}}{e^{\frac{\pi v}{2u_m}} + e^{-\frac{\pi v}{2u_m}}} \tag{4}$$

Thus, the actuator saturation model is re-described as:

$$sat(v) = g(v) + d(v) \tag{5}$$

where $g(v)$ is a smooth function. $d(v) = sat(v) - g(v)$ is a bounded function. Inspired by Yang et al.,[54] it can be expressed as:

$$|d(v)| = |sat(v) - g(v)| \leqslant u_m(1 - \tanh(1)) = \bar{d} \tag{6}$$

where $\bar{d}$ is a positive constant.

According to the **Mean Value Theorem**, the above-segmented function can be rewritten as:

$$g(v) = g_{v_\mu}(v - v_0) + g(v_0) \tag{7}$$

where $0 < \mu < 1, g_{v_\mu} = \frac{\partial g(v)}{\partial v}\Big|_v = v_\mu$ and $v_\mu = \mu v + (1-\mu)v_0$.

By choosing $v_0 = 0$, it can be verified that $g(v) = g_{v_\mu}\mu$. Thus, we can further obtain

$$u = d(v) + g v_\mu v \tag{8}$$

Remark 2: By the definition of (v), similar to Mu et al.,[55] it is known that the definition of the normal number $\underline{g}$ and $\bar{g}$ satisfies $\underline{g} \leqslant g_{v_\mu} \leqslant \bar{g}, v \in R$.

Multi-dimensional Taylor network

In the design process of the controller, MTNs are used to approximate the unknown nonlinearity that occurs in the system. The following lemma is stated for function approximation.

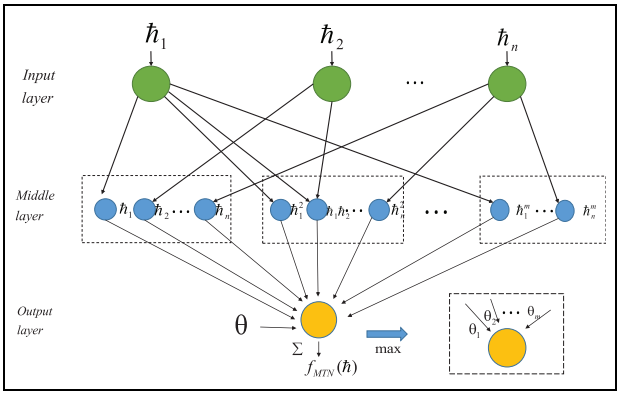

Figure 1. The structure diagram of MTN.

Lemma 1.[43] Suppose $H(\hbar_1, \ldots, \hbar_n) : R^n \to R$ is a function defined in the closed interval $\Omega \subset R^n$, for any given constant $\bar{\varepsilon} > 0$, there exists an MTN with an approximation error $\varepsilon(\hbar)$ satisfying the

$$H(\hbar) = \boldsymbol{\theta}^T\varphi(\hbar) + \varepsilon(\boldsymbol{h}), |\varepsilon(\hbar)| \leqslant \bar{\varepsilon} \tag{9}$$

where $\hbar = [\hbar_1, \ldots, \hbar_n]^T \in R^n$ and $\boldsymbol{\theta} = [\theta_1, \ldots, \theta_l]^T \in R^l$ are the input vector and the weight vector of MTN, respectively. $\varphi(\hbar) = [\hbar_1, \cdots, \hbar_n, \hbar_1^2, \hbar_1\hbar_2, \cdots, \hbar_n^2, \cdots, \hbar_1^m, \cdots, \hbar_n^m]^T \in R^l$ denotes the middle layer.

Remark 3: As illustrated in Figure 1, MTN is a three-layer feedforward neural network comprising the input layer, the middle layer, and the output layer. For more information about MTN, the reader can refer to He et al.,[40] Li et al.,[41] Han and Sun,[56] Wang et al.,[44,57] and Lu et al.[58]

Error transformation

Since the presence of multiple sensor faults makes all state variables $x_i(t)$ unavailable, the following coordinate changes are introduced

$$\begin{aligned} z_1 &= x_1 - y_d = \hat{l}_1 x_1^f - y_d + \tilde{l}_1 x_1^f = \tilde{z}_1 + \tilde{l}_1 x_1^f \\ z_i &= x_i - \alpha_{i-1} = \hat{l}_i x_1^f - \alpha_{i-1} + \tilde{l}_i x_1^f = \tilde{z}_i + \tilde{l}_i x_1^f \end{aligned} \tag{10}$$

where $\alpha_i - 1$ is the virtual control function, $l_i = \frac{1}{\rho_i}$ and $\hat{l}_i$ is estimate of l_i with $\tilde{l}_i = l_i - \hat{l}_i$

Inspired by Zhang and Yang,[59] due to the presence of multiple sensor faults, the available error signal $z_i^f = x_i^f - \alpha_{i-1}$ has been corrupted and cannot be used directly as a feedback signal, the compensation signal $\hat{l}_i x_i^f$ is introduced to mitigate the effects of sensor faults. Therefore, the compensation error $\tilde{z}_i$ is to be used instead of z_i.

To achieve control objectives, the following Assumptions and Lemma are needed, which will play an important role in the controller design process.

Assumption 1: In system (1), for bounded uncertainty, the inequality $|\Delta_i| \leqslant \bar{\Delta}_i$ holds, where $\bar{\Delta}_i$ is a positive constant.

Assumption 2: The desired trajectory y_d is a known smooth bounded signal and its time derivatives up to the n-th order are continuous.

Lemma 2.[4] The cubic absolute value function $\Xi(\chi(t)) = \frac{1}{3}|\chi(t)|^3$ is differentiable and its time derivative is $\dot{\Xi}(\chi(t)) = \chi^2\dot{\chi}sign(\chi)$.

Main results

Controller design

Due to error conversion provided by (10), the design of the intermediate control signal and the controller will be carried out in the following n steps.

Step 1: Construct a cubic absolute value Lyapunov candidate function as:

$$V_1 = \frac{1}{2}z_1^2 + \frac{1}{2\eta}\tilde{\boldsymbol{\theta}}_1^T\tilde{\boldsymbol{\theta}}_1 + \frac{1}{3r}\left|\tilde{l}_1\right|^3 \tag{11}$$

where $\eta > 0, r > 0$ is the parameter to be designed. $\boldsymbol{\theta}_1$ is a vector provided in the subsequent design. Write $\hat{\boldsymbol{\theta}}_1$ as an estimate of $\boldsymbol{\theta}_1$ along with $\tilde{\boldsymbol{\theta}}_1 = \boldsymbol{\theta}_1 - \hat{\boldsymbol{\theta}}_1$.

According to Lemma 2, the time-derivative of V_1 can be computed as

$$\begin{aligned}\dot{V}_1 = {} & z_1[\alpha_1 + z_2 + \Delta_1 + H_1(\boldsymbol{Z}_1)] \\ & -\frac{1}{\eta}\tilde{\boldsymbol{\theta}}_1^T\dot{\hat{\boldsymbol{\theta}}}_1 - \frac{1}{r}\tilde{l}_1^2\dot{\hat{l}}_1 sign(\tilde{l}_1)\end{aligned} \tag{12}$$

where $H_1(\boldsymbol{Z}_1) = f_1(\bar{\boldsymbol{x}}_1) - \dot{y}$ is an unknown function.

By applying Lemma 1, one has

$$H_1(\boldsymbol{Z}_1) = \boldsymbol{\theta}_1^T\varphi_1(\boldsymbol{Z}_1) + \varepsilon_1(\boldsymbol{Z}_1), |\varepsilon_1(\boldsymbol{Z}_1)| \leqslant \bar{\varepsilon}_1 \tag{13}$$

where $\boldsymbol{Z}_1 = [\boldsymbol{x}_1^f, \hat{\boldsymbol{l}}_1, \dot{\boldsymbol{y}}_d]^T$, $\boldsymbol{\theta}_1$ is ideal weight vector, and $\forall\bar{\varepsilon}_1 > 0$ is a bounded approximation error.

By applying Young's inequality, the following inequality holds

$$\begin{aligned}z_1\varepsilon_1 + z_1z_2 + z_1\Delta_1 &\leqslant \frac{3}{2}z_1^2 + \frac{1}{2}\varepsilon_1^2 + \frac{1}{2}z_2^2 + \frac{1}{2}\Delta_1^2 \\ &\leqslant \frac{3}{2}z_1^2 + \frac{1}{2}\bar{\varepsilon}_1^2 + \frac{1}{2}z_2^2 + \frac{1}{2}\bar{\Delta}_1^2\end{aligned} \tag{14}$$

Substituting (13) and (14) into (12) results in

$$\begin{aligned}\dot{V}_1 \leqslant {} & z_1\alpha_1 + \frac{3}{2}z_1^2 + \frac{1}{2}\bar{\varepsilon}_1^2 + \frac{1}{2}z_2^2 + \frac{1}{2}\bar{\Delta}_1^2 + z_1\boldsymbol{\theta}_1^T\varphi_1 \\ & -\frac{1}{\eta}\tilde{\boldsymbol{\theta}}_1^T\dot{\hat{\boldsymbol{\theta}}}_1 - \frac{1}{r}\tilde{l}_1^2\dot{\hat{l}}_1 sign(\tilde{l}_1)\end{aligned} \tag{15}$$

According to (15), the intermediate control signal is designed as follows

$$\alpha_1 = -c_1\tilde{z}_1 - \hat{\boldsymbol{\theta}}_1^T\varphi_1(\boldsymbol{Z}_1) \tag{16}$$

where $c_1 > 0$ is a parameter to be designed.

Substituting (16) into (15) results in

$$\begin{aligned}\dot{V}_1 \leqslant {} & -c_1z_1\tilde{z}_1 - z_1\hat{\boldsymbol{\theta}}_1^T\varphi_1(\boldsymbol{Z}_1) + \frac{3}{2}z_1^2 + \frac{1}{2}\bar{\varepsilon}_1^2 + \frac{1}{2}z_2^2 \\ & + \frac{1}{2}\bar{\Delta}_1^2 + z_1\boldsymbol{\theta}_1^T\varphi_1 - \frac{1}{\eta}\tilde{\boldsymbol{\theta}}_1^T\dot{\hat{\boldsymbol{\theta}}}_1 - \frac{1}{r}\tilde{l}_1^2\dot{\hat{l}}_1 sign(\tilde{l}_1) \\ = {} & c_1z_1\tilde{z}_1 + z_1\tilde{\boldsymbol{\theta}}_1^T\varphi_1 + \frac{3}{2}z_1^2 + \frac{1}{2}\bar{\varepsilon}_1^2 + \frac{1}{2}z_2^2 + \frac{1}{2}\bar{\Delta}_1^2 \\ & -\frac{1}{\eta}\tilde{\boldsymbol{\theta}}_1^T\dot{\hat{\boldsymbol{\theta}}}_1 - \frac{1}{r}\tilde{l}_1^2\dot{\hat{l}}_1 sign(\tilde{l}_1)\end{aligned} \tag{17}$$

By trigonometric inequality, the following two inequalities hold

$$\begin{aligned}-c_1z_1\tilde{z}_1 = {} & -c_1z_1(z_1 - \tilde{l}_1x_1^f) \\ = {} & -c_1z_1^2 + c_1\tilde{l}_1x_1^f(\tilde{z}_1 + \tilde{l}_1x_1^f) \\ \leqslant {} & -c_1z_1^2 + \xi(c_1\tilde{l}_1x_1^f)^2 + \frac{1}{4\xi} + c_1(\tilde{l}_1x_1^f)^2\end{aligned} \tag{18}$$

$$\begin{aligned}z_1\tilde{\boldsymbol{\theta}}_1^T\varphi_1(\boldsymbol{Z}_1) = {} & (\tilde{z}_1 + 1_1x_1^f)\tilde{\boldsymbol{\theta}}_1^T\varphi_1(\boldsymbol{Z}_1) \\ \leqslant {} & \tilde{z}_1\tilde{\boldsymbol{\theta}}_1^T\varphi_1(\boldsymbol{Z}_1) + \frac{1}{2}(\tilde{l}_1x_1^f)^2 \parallel \varphi_1(\boldsymbol{Z}_1)\|^2 \\ & + \frac{1}{2}\tilde{\boldsymbol{\theta}}_1^T\tilde{\boldsymbol{\theta}}_1\end{aligned} \tag{19}$$

where $\xi > 0$ is a parameter to be designed.

From (17), (18), and (19), it yields

$$\begin{aligned}\dot{V}_1 \leqslant {} & -C_1z_1^2 + \xi\left(c_1\tilde{l}_1x_1^f\right)^2 + \frac{1}{4\xi} + c_1\left(\tilde{l}_1x_1^f\right)^2 \\ & + \tilde{z}_1\tilde{\boldsymbol{\theta}}_1^T\varphi_1(\boldsymbol{Z}_1) + \frac{1}{2}\left(\tilde{l}_1x_1^f\right)^2 \parallel \varphi_1(\boldsymbol{Z}_1)\|^2 \\ & + \frac{1}{2}\tilde{\boldsymbol{\theta}}_1^T\tilde{\boldsymbol{\theta}}_1 - \frac{1}{\eta}\tilde{\boldsymbol{\theta}}_1^T\dot{\hat{\boldsymbol{\theta}}}_1 + \frac{1}{2}\bar{\varepsilon}_1^2 + \frac{1}{2}z_2^2 + \frac{1}{2}\bar{\Delta}_1^2 \\ & -\frac{1}{r}\tilde{l}_1^2\dot{\hat{l}}_1 sign(\tilde{l}_1)\end{aligned} \tag{20}$$

where $C_1 = c_1 - \frac{3}{2} > 0$ is the parameter to be designed.

Based on (20), design the adaptive laws are as follows

$$\dot{\hat{\boldsymbol{\theta}}}_1 = \eta \tilde{z}_1 \varphi_1(\boldsymbol{Z}_1) - \eta\sigma\hat{\boldsymbol{\theta}}_1 \tag{21}$$

$$\dot{\hat{l}}_1 = \begin{cases} r\left[\xi c_1^2 \tilde{z}_1^2 + c_1 + \frac{1}{2}\right]\left(x_1^f\right)^2 - r\bar{\sigma}_1 \hat{l}_1, & m_1 > 0 \\ 0, & m_1 \leqslant 0 \end{cases} \tag{22}$$

where $m_1 = r\left[\xi c_1^2 \tilde{z}_1^2 + c_1 + \frac{1}{2}\right]\left(x_1^f\right)^2 - r\bar{\sigma}_1 \hat{l}_1$, σ and $\bar{\sigma}_1$ are positive design parameters.

Substituting (21) and (22) into (20), we can obtain

$$\begin{aligned} \dot{V}_1 \leqslant & -C_1 z_1^2 + \frac{1}{2}\tilde{\boldsymbol{\theta}}_1^T \tilde{\boldsymbol{\theta}}_1 - \sigma \tilde{\boldsymbol{\theta}}_1^T \tilde{\boldsymbol{\theta}}_1 - \bar{\sigma}_1 \tilde{l}_1^2 \hat{l}_1 sign\left(\tilde{l}_1\right) \\ & + \frac{1}{2} z_2^2 + D_1 \end{aligned} \tag{23}$$

where $D_1 = \frac{1}{4\xi} + \frac{1}{2}\bar{\varepsilon}_2^2 + \frac{1}{2}\bar{\Delta}_1^2$.

Step $i (2 \leqslant i \leqslant n-1)$: Construct a cubic absolute-value Lyapunov candidate V_i as follows

$$V_i = V_{i-1} + \frac{1}{2} z_i^2 + \frac{1}{2\eta}\tilde{\boldsymbol{\theta}}_i^T \tilde{\boldsymbol{\theta}}_i + \frac{1}{3r}\left|\tilde{l}_i\right|^3 \tag{24}$$

where $\tilde{\boldsymbol{\theta}}_i = \boldsymbol{\theta}_i - \hat{\boldsymbol{\theta}}_i$, and $\boldsymbol{\theta}_i$ and $\hat{\boldsymbol{\theta}}_i$ are the weight vector and its estimate.

According to Lemma 2, the time-derivative of V_i can be computed as

$$\begin{aligned} \dot{V}_i &= \dot{V}_{i-1} + z_i[x_{i+1} + f_i(\bar{\boldsymbol{x}}_i) + \Delta_i - \dot{\alpha}_{i-1}] \\ &\quad - \frac{1}{\eta}\tilde{\boldsymbol{\theta}}_i^T \dot{\hat{\boldsymbol{\theta}}}_i - \frac{1}{r}\tilde{l}_i^2 \hat{\boldsymbol{\theta}}_i sign\left(\tilde{l}_i\right) \\ &= \dot{V}_{i-1} + z_i\left[\alpha_i + z_{i+1} + \Delta_i - \frac{1}{2} z_i + H_i(\boldsymbol{Z}_i)\right] \\ &\quad - \frac{1}{\eta}\tilde{\boldsymbol{\theta}}_i^T \dot{\hat{\boldsymbol{\theta}}}_i - \frac{1}{r}\tilde{l}_i^2 \hat{\boldsymbol{\theta}}_i sign\left(\tilde{l}_i\right) \end{aligned} \tag{25}$$

where $H_i(\boldsymbol{Z}_i) = \left[f_i(\bar{\boldsymbol{x}}_i) - \dot{\alpha}_{i-1} + \frac{z_i}{2}\right]$ is an unknown function.

According to Lemma 1, for $\forall \bar{\varepsilon}_i > 0$, one has

$$H_i(\boldsymbol{Z}_i) = \boldsymbol{\theta}_i^T \varphi_i(\boldsymbol{Z}_i) + \varepsilon_i(\boldsymbol{Z}_i), |\varepsilon_i(\boldsymbol{Z}_i)| \leqslant \bar{\varepsilon}_i \tag{26}$$

where $\boldsymbol{Z}_i = \left[\boldsymbol{x}_i^f, \hat{\boldsymbol{\theta}}_{i-1}, \boldsymbol{y}_d^{(i)}, \hat{\boldsymbol{l}}_i\right]^T$, $\boldsymbol{x}_i^f = \left[x_1^f, x_2^f, \ldots, x_i^f\right]^T$, $\hat{\boldsymbol{\theta}}_{i-1} = \left[\hat{\theta}_1^T, \hat{\theta}_2^T, \ldots, \hat{\theta}^T{}_{i-1}\right]^T$, $\boldsymbol{y}_d^{(i)} = \left[\dot{y}_d, \ldots, y_d^{(i)}\right]^T$, $\hat{\boldsymbol{l}}_i = \left[\hat{l}_1, \hat{l}_2, \ldots, \hat{l}_i\right]^T$, and $\varepsilon_i(\boldsymbol{Z}_i)$ is a bounded approximation error.

According to Young's inequality, the following inequality holds

$$\begin{aligned} z_i\varepsilon_i + z_i z_{i+1} + z_i\Delta_i &\leqslant \frac{3}{2} z_i^2 + \frac{1}{2}\varepsilon_i^2 + \frac{1}{2} z_{i+1}^2 + \frac{1}{2}\Delta_i^2 \\ &\leqslant \frac{3}{2} z_i^2 + \frac{1}{2}\bar{\varepsilon}_i^2 + \frac{1}{2} z_{i+1}^2 + \frac{1}{2}\bar{\Delta}_i^2 \end{aligned} \tag{27}$$

Substituting (26) and (27) into (25) results in

$$\begin{aligned} \dot{V}_i = \dot{V}_{i-1} &+ z_i\alpha_i + z_i\boldsymbol{\theta}_i{}^T\varphi_i + \frac{1}{2}\bar{\varepsilon}_i^2 + z_i^2 + \frac{1}{2} z_{i+1}^2 \\ &+ \frac{1}{2}\bar{\Delta}_i^2 - \frac{1}{\eta}\tilde{\boldsymbol{\theta}}_i^T \dot{\hat{\boldsymbol{\theta}}}_i - \tilde{l}_i^2 \dot{\hat{l}}_i sign\left(\tilde{l}_i\right) \end{aligned} \tag{28}$$

Based on (28), design the virtual controller α_i as follows

$$\alpha_i = -c_i\tilde{z}_i - \hat{\boldsymbol{\theta}}_i^T \varphi_i(\boldsymbol{Z}_i) \tag{29}$$

where $c_i > 0$ is a parameter to be designed.

Substituting (29) into (28) results in

$$\begin{aligned} \dot{V}_i &= \dot{V}_{i-1} - c_i z_i \tilde{z}_i - z_i\hat{\boldsymbol{\theta}}_i^T\varphi_i + z_i\boldsymbol{\theta}_i^T\varphi_i + \frac{1}{2}\bar{\varepsilon}_i^2 \\ &\quad + z_i^2 + \frac{1}{2} z_{i+1}^2 - \frac{1}{\eta}\tilde{\boldsymbol{\theta}}_i^T\dot{\hat{\boldsymbol{\theta}}}_i - \frac{1}{r}\tilde{l}_i^2\hat{\boldsymbol{\theta}}_i sign\left(\tilde{l}_i\right) \\ &= \dot{V}_{i-1} - c_i z_i \tilde{z}_i + z_i\tilde{\boldsymbol{\theta}}_i^T\varphi_i + \frac{1}{2}\bar{\Delta}_i^2 + z_i^2 + \frac{1}{2}\bar{\Delta}_i^2 \\ &\quad + \frac{1}{2} z_{i+1}^2 - \frac{1}{\eta}\tilde{\boldsymbol{\theta}}_i^T\dot{\hat{\boldsymbol{\theta}}}_i - \frac{1}{r}\tilde{l}_i^2\hat{\boldsymbol{\theta}}_i sign\left(\tilde{l}_i\right) \end{aligned} \tag{30}$$

By trigonometric inequality, the following two inequalities hold

$$\begin{aligned} -c_i z_i\tilde{z}_i &= -c_i z_i\left(z_i - \tilde{l}_i x_i^f\right) \\ &= -c_i z_i^2 + c_i\tilde{l}_i x_i^f\left(\tilde{z}_i + \tilde{l}_i x_i^f\right) \\ &\leqslant -c_i z_i^2 + \xi\left(c_i\tilde{l}_i x_i^f\right)^2 + \frac{1}{4\xi} + c_i\left(\tilde{l}_i x_i^f\right)^2 \end{aligned} \tag{31}$$

$$\begin{aligned} z_i\theta_i^T\varphi_i\left(\boldsymbol{x}_i^f\right) &= \left(\tilde{z}_i + \tilde{l}_i\boldsymbol{x}_i^f\right)\tilde{\theta}_i^T\varphi_i(\boldsymbol{Z}_i) \\ &\leqslant \tilde{z}_i\tilde{\theta}_i^T\varphi_i(\boldsymbol{Z}_i) + \frac{1}{2}\left(\tilde{l}_i\boldsymbol{x}_i^f\right)^2 \| \varphi_i(\boldsymbol{Z}_i)\|^2 \\ &\quad + \frac{1}{2}\tilde{\boldsymbol{\theta}}_i^T\tilde{\boldsymbol{\theta}}_i \end{aligned} \tag{32}$$

From (30), (31), and (32), it yields

$$\dot{V}_i \leqslant \dot{V}_{i-1} - C_i z_i^2 + \xi\left(c_i \tilde{l}_i x_i^f\right)^2 + \frac{1}{4\xi} + c_i\left(\tilde{l}_i x_i^f\right)^2 + \tilde{z}_i \tilde{\boldsymbol{\theta}}_i^T \varphi_i + \frac{1}{2}\left(\tilde{l}_i x_i^f\right)^2 + \frac{1}{2}\tilde{\boldsymbol{\theta}}_i^T \tilde{\boldsymbol{\theta}}_i - \frac{1}{2} z_i^2 + \frac{1}{2}\bar{\varepsilon}_i^2 + \frac{1}{2} z_{i+1}^2 + \frac{1}{2}\bar{\Delta}_i^2 - \frac{1}{\eta}\tilde{\boldsymbol{\theta}}_i^T \dot{\hat{\boldsymbol{\theta}}}_i - \frac{1}{r}\tilde{l}_i^2 \dot{\hat{l}}_i sign\left(\tilde{l}_i\right) \tag{33}$$

where $C_i = c_i - \frac{3}{2} > 0$ is the parameter to be designed.

Based on (33), design the adaptive parameter $\hat{\boldsymbol{\theta}}_i$ and $\hat{l}_i$ as

$$\dot{\hat{\boldsymbol{\theta}}}_i = \eta \tilde{z}_i \varphi_i(\boldsymbol{Z}_i) - \eta\sigma\hat{\boldsymbol{\theta}}_i \tag{34}$$

$$\dot{\hat{l}}_i = \begin{cases} r\left[\xi c_i^2 \tilde{z}_i^2 + c_i + \frac{1}{2}\right]\left(x_i^f\right)^2 - r\bar{\sigma}_i \hat{l}_i, & m_i > 0 \\ 0, & m_i \leqslant 0 \end{cases} \tag{35}$$

where $m_i = r\left[\xi c_i^2 \tilde{z}_i^2 + c_i + \frac{1}{2}\right](x_i^f)^2 - r\bar{\sigma}_i \hat{l}_i$, σ and $\bar{\sigma}_i$ are positive design parameters.

Substituting (34) and (35) into (33) yields

$$\dot{V}_i \leqslant \sum_{j=1}^{i}\Big[-C_j z_j^2 + \frac{1}{2}\tilde{\boldsymbol{\theta}}_j^T \tilde{\boldsymbol{\theta}}_j - \sigma \tilde{\boldsymbol{\theta}}_j^T \hat{\boldsymbol{\theta}}_j - \bar{\sigma}_j \tilde{l}_j^2 \dot{\hat{l}}_j sign\left(\tilde{l}_j\right)\Big] + \frac{1}{2} z_{j+1}^2 + D_j \tag{36}$$

where $D_i = D_{i-1} + \frac{1}{4\xi} + \frac{1}{2}\bar{\varepsilon}_i^2 + \frac{1}{2}\bar{\Delta}_i^2$.

Step n: According to (1) and (8), $\dot{x}_n$ can be calculated as follows

$$\dot{x}_n = g_{v_\mu} v + d(v) + f_n(\bar{x}_n) + \Delta_n(t) \tag{37}$$

Choose the Lyapunov candidate V_n as follows

$$V_n = V_{n-1} + \frac{1}{2} z_n^2 + \frac{1}{2\eta}\tilde{\boldsymbol{\theta}}_n^T \tilde{\boldsymbol{\theta}}_n + \frac{1}{3r}\left|\tilde{l}_n\right|^3 \tag{38}$$

where $\boldsymbol{\theta}_\mathbf{n}$ is a vector provided in the subsequent design. Write $\hat{\boldsymbol{\theta}}_n$ as an estimate of $\boldsymbol{\theta}_n$ along with $\tilde{\boldsymbol{\theta}}_n = \boldsymbol{\theta}_n - \hat{\boldsymbol{\theta}}_n$.

According to Lemma 2, the time-derivative of V_n can be computed as

$$\begin{aligned} \dot{V}_n &= \dot{V}_{n-1} + z_n - \frac{1}{\eta}\tilde{\boldsymbol{\theta}}_n^T \dot{\hat{\boldsymbol{\theta}}}_n - \frac{1}{r}\tilde{l}_n^2 \dot{\hat{l}}_n sign\left(\tilde{l}_n\right) \\ &= \dot{V}_{n-1} + z_n\left(g_{v_\mu} v + d(v) + f_n + \Delta_n - \dot{\alpha}_{n-1}\right) - \frac{1}{\eta}\tilde{\boldsymbol{\theta}}_n^T \dot{\hat{\boldsymbol{\theta}}}_n - \frac{1}{r}\tilde{l}_n^2 \dot{\hat{l}}_n sign\left(\tilde{l}_n\right) \\ &= \dot{V}_{n-1} + z_n\left(g_{v_\mu} v + d(v) + \Delta_n + H_n - \frac{1}{2} z_n\right) - \frac{1}{\eta}\tilde{\boldsymbol{\theta}}_n^T \dot{\hat{\boldsymbol{\theta}}}_n - \frac{1}{r}\tilde{l}_n^2 \dot{\hat{l}}_n sign\left(\tilde{l}_n\right) \end{aligned} \tag{39}$$

where $H_n(\boldsymbol{Z}_n) = \left[f_n(\bar{\boldsymbol{x}}_n) - \dot{\alpha}_{n-1} + \frac{z_n}{2}\right]$ is an unknown function.

By applying MTN to approximate $H_n(\boldsymbol{Z}_n)$, for $\forall \bar{\varepsilon}_n > 0$, one has

$$H_n(\boldsymbol{Z}_n) = \boldsymbol{\theta}_n^T \varphi_n(\boldsymbol{Z}_n) + \varepsilon_n(\boldsymbol{Z}_n), |\varepsilon_n(\boldsymbol{Z}_n)| \leqslant \bar{\varepsilon}_n \tag{40}$$

where $\boldsymbol{Z}_n = [\boldsymbol{x}_n^f, \hat{\boldsymbol{\theta}}_n, \hat{\boldsymbol{l}}_n, \boldsymbol{y}_d^{(n)}]^T$ with $\boldsymbol{x}_n^f = [x_1^f, x_2^f, \ldots, x_n^f]^T$, $\hat{\boldsymbol{\theta}}_n = [\hat{\theta}_1^T, \hat{\theta}_2^T, \ldots, \hat{\theta}^T{}_n]^T$, $\hat{\boldsymbol{l}}_n = [\hat{l}_1, \hat{l}_2, \ldots, \hat{l}_n]^T$ and $\boldsymbol{y}_d^{(n)} = [y_d, \ldots, y_d^{(n)}]^T$. $\boldsymbol{\theta}_n$ is ideal weight vector, and $\varepsilon_n(\boldsymbol{Z}_n)$ is a bounded approximation error.

Substituting (40) into (39) results in

$$\begin{aligned} \dot{V}_n &= V_{n-1} + z_n\left(g_{v_\mu} v + d + f_n + \Delta_n - \dot{\alpha}_{n-1}\right) - \frac{1}{\eta}\tilde{\boldsymbol{\theta}}_n^T \dot{\hat{\boldsymbol{\theta}}}_n - \frac{1}{r}\tilde{l}_n^2 \dot{\hat{l}}_n sign\left(\tilde{l}_n\right) \\ &= \dot{V}_{n-1} + z_n(g_{v_\mu} v + d + \Delta_n + \boldsymbol{\theta}_n^T \varphi_n + \varepsilon_n - \frac{z_n}{2}) - \frac{1}{\eta}\tilde{\boldsymbol{\theta}}_n^T \dot{\hat{\boldsymbol{\theta}}}_n - \frac{1}{r}\tilde{l}_n^2 \dot{\hat{l}}_n sign\left(\tilde{l}_n\right) \end{aligned} \tag{41}$$

By applying Young's inequality the following inequality holds:

$$\begin{aligned} z_n\varepsilon_n + z_n\Delta_n(t) + z_n d &\leqslant \frac{1}{2} z_n^2 + \frac{1}{2}\bar{\varepsilon}_n^2 + \frac{1}{2} z_n^2 + \frac{1}{2}\bar{d}^2 + \frac{1}{2}\bar{\Delta}_n^2(t) + \frac{1}{2} z_n^2 \\ &= \frac{3}{2} z_n^2 + \frac{1}{2}\bar{\varepsilon}_n^2 + \frac{1}{2}\bar{\Delta}_n^2(t) + \frac{1}{2}\bar{d}^2 \end{aligned} \tag{42}$$

Substituting (42) into (41), we have

$$\dot{V}_n = \dot{V}_{n-1} + z_n g_{v_\mu} v + z_n \boldsymbol{\theta}_n^T \varphi_n + z_n^2 + \frac{1}{2}\bar{\varepsilon}_n^2 + \frac{1}{2}\bar{d}^2 + \frac{1}{2}\bar{\Delta}_n^2 - \frac{1}{\eta}\tilde{\boldsymbol{\theta}}_n^T \dot{\hat{\boldsymbol{\theta}}}_n - \frac{1}{r}\tilde{l}_n^2 \dot{\hat{l}}_n sign\left(\tilde{l}_n\right) \tag{43}$$

Based on (43), design the actual controller v as follows

$$v = -\frac{1}{\underline{g}}\left(c_n \tilde{z}_n + \hat{\boldsymbol{\theta}}_n^T \varphi_n(\boldsymbol{Z}_n)\right) \tag{44}$$

where c_n is a positive constant.

Substituting (44) into (43) result in

$$\dot{V}_n = \dot{V}_{n-1} - c_n \frac{g_{v_\mu}}{\underline{g}} z_n \tilde{z}_n + z_n \tilde{\boldsymbol{\theta}}_n^T \varphi_n + \frac{z_n^2}{2} + \frac{1}{2}\bar{\varepsilon}_n^2 + \frac{1}{2}\bar{\Delta}_n^2 - \frac{1}{\eta}\tilde{\boldsymbol{\theta}}_n^T \dot{\hat{\boldsymbol{\theta}}}_n - \frac{1}{r}\tilde{l}_n^2 \dot{\hat{l}}_n sign\left(\tilde{l}_n\right) \tag{45}$$

By trigonometric inequality, the following two inequalities hold

$$\begin{aligned} z_n\tilde{\boldsymbol{\theta}}_n^T\varphi_n(x_n^f) &= \left(\tilde{z}_n + \tilde{l}_n x_n^f\right)\tilde{\boldsymbol{\theta}}_n^T\varphi_n(\boldsymbol{Z}_n) \\ &\leqslant \frac{1}{2}\left(\tilde{l}_n x_n^f\right)^2 \parallel \varphi_n\parallel^2 + \tilde{z}_n\tilde{\boldsymbol{\theta}}_n^T\varphi_n \end{aligned} \tag{46}$$

$$\begin{aligned} c_n\frac{g_{v_\mu}}{\underline{g}}z_n\tilde{z}_n &= -c_n\frac{g_{v_\mu}}{\underline{g}}\left[z_n\left(z_n-\tilde{l}_n x_n^f\right)\right] \\ &= -c_n\frac{g_{v_\mu}}{\underline{g}}z_n^2 + c_n\frac{g_{v_\mu}}{\underline{g}}\tilde{l}_n x_n^f\left(\tilde{z}_n+\tilde{l}_n x_n^f\right) \\ &\leqslant -c_n z_n^2 + c_n\frac{g_{v_\mu}}{\underline{g}}\tilde{l}_n x_n^f\tilde{z}_n + c_n\frac{g_{v_\mu}}{\underline{g}}\left(\tilde{l}_n x_n^f\right)^2 \\ &\leqslant -c_n z_n^2 + c_n\frac{\bar{g}}{\underline{g}}\tilde{l}_n x_n^f\tilde{z}_n + c_n\frac{\bar{g}}{\underline{g}}\left(\tilde{l}_n x_n^f\right)^2 \\ &\leqslant -c_n z_n^2 + \xi\left(c_n\frac{\bar{g}}{\underline{g}}\tilde{l}_n x_n^f\tilde{z}_n\right)^2 + \frac{1}{4\xi} \\ &\quad + c_n\left(\tilde{l}_n x_n^f\right)^2 \end{aligned} \tag{47}$$

Substituting (46) and (47) into (45) results in

$$\begin{aligned} \dot{V}_n = \dot{V}_{n-1} &- c_n z_n^2 + \xi\left(c_n\tilde{z}_n\tilde{l}_n x_n^f\right)^2 + \frac{1}{4\xi} + \frac{1}{2}\bar{\varepsilon}_n^2 \\ &+ c_n\left(\tilde{l}_n x_n^f\right)^2 + \tilde{z}_n\tilde{\boldsymbol{\theta}}_n^T\varphi_n - \frac{1}{r}\tilde{l}_n^2\dot{\hat{l}}_n sign\left(\tilde{l}_n\right) \\ &+ \frac{1}{2}\left(\tilde{l}_n x_n^f\right)^2 + \frac{1}{2}\bar{\Delta}_n^2 - \frac{1}{\eta}\tilde{\boldsymbol{\theta}}_n^T\dot{\hat{\boldsymbol{\theta}}}_n + \frac{1}{2}\tilde{\boldsymbol{\theta}}_n^T\tilde{\boldsymbol{\theta}}_n \end{aligned} \tag{48}$$

where $C_n = c_n - \frac{3}{2} > 0$ is a parameter to be designed.

According to (48), design the adaptive parameters $\hat{\boldsymbol{\theta}}_n$ and $\hat{\boldsymbol{l}}_n$ as follows

$$\dot{\hat{\boldsymbol{\theta}}}_n = \eta\tilde{z}_n\varphi_n(\boldsymbol{Z}_n) - \eta\sigma\hat{\boldsymbol{\theta}}_n \tag{49}$$

$$\dot{\hat{l}}_n = \begin{cases} r\left[\xi c_n\tilde{z}_n^2 + c_n + \frac{1}{2}\right]\left(x_n^f\right)^2 - r\bar{\sigma}_n\hat{l}_n, & m_n > 0 \\ 0, & m_n \leqslant 0 \end{cases} \tag{50}$$

where $m_n = r\left[\xi c_n^2\tilde{z}_n^2 + c_n + \frac{n}{2}\right]\left(x_n^f\right)^2 - r\bar{\sigma}_n\hat{l}_n$, σ and $\bar{\sigma}_n$ are positive design parameters.

Then, substituting (49) and (50) into (48), we have

$$\dot{V}_n \leqslant \sum_{i=1}^{n}\left[-C_n z_n^2 + \tfrac{1}{2}\tilde{\boldsymbol{\theta}}_n^T\tilde{\boldsymbol{\theta}}_n - \sigma\tilde{\boldsymbol{\theta}}_n^T\hat{\boldsymbol{\theta}}_n - \bar{\sigma}_n\left|\tilde{l}_n\right|^3\right] + D_n \tag{51}$$

where $D_n = D_{n-1} + \sum_{i=1}^{n}\left(\frac{\sigma}{2}\boldsymbol{\theta}_n^T\boldsymbol{\theta}_n + \frac{\bar{\sigma}_n}{3}l_n^3\right) + \frac{1}{2}\bar{\Delta}_n^2$.

Stability analysis

The above design and analysis process can be summarized in the following theorem.

Theorem 1: Under Assumptions 1, consider the closed-loop system (1) under multiple sensor fault (3) and actuator saturation (2). Then the actual controller (44) and the virtual controllers (16), (29) with adaptive laws (21), (22), (34), (35), (49), and (50) can guarantee that (i) the boundedness of all the signals in the controlled system; (ii) The system output y can follow the desired reference signal y_d efficiently. Further, the tracking error $|y(t) - y_d(t)|$ can be arbitrarily small by choosing appropriate controller parameters.

Proof: For the closed-loop system, consider Lyapunov function $V = V_n$. According to (51), we have

$$\dot{V} \leqslant \sum_{i=1}^{n}\left[-C_n z_n^2 + \tfrac{1}{2}\tilde{\boldsymbol{\theta}}_n^T\tilde{\boldsymbol{\theta}}_n - \sigma\tilde{\boldsymbol{\theta}}_n^T\hat{\boldsymbol{\theta}}_n - \bar{\sigma}_n\left|\tilde{l}_n\right|^3\right] + D_n \tag{52}$$

According to (22), (35), and (50), and using the similar analysis in Zhang and Yang,[59] we have

$$\tilde{l}_n^2\hat{l}_n sign\left(\tilde{l}_n\right) = \tilde{l}_n^2\hat{l}_n \leqslant -\frac{1}{3}\left|\tilde{l}_n\right|^3 + \frac{1}{3}l_n^3 \tag{53}$$

On the other hand, according to the definition of $\tilde{\boldsymbol{\theta}}$ and $\hat{\boldsymbol{\theta}}_n$, we have

$$\tilde{\boldsymbol{\theta}}_n^T\hat{\boldsymbol{\theta}}_n \leqslant -\frac{1}{2}\tilde{\boldsymbol{\theta}}_n^T\tilde{\boldsymbol{\theta}}_n + \frac{1}{2}\boldsymbol{\theta}_n^T\boldsymbol{\theta}_n \tag{54}$$

Substituting the (53) and (54) into (51) results in

$$\dot{V} \leqslant \sum_{i=1}^{n}\left[-C_n z_n{}^2 - \left(\sigma - \frac{1}{2}\right)\tilde{\boldsymbol{\theta}}_n{}^T\tilde{\boldsymbol{\theta}}_n - \bar{\sigma}_n\left|\tilde{l}_n\right|^3\right] + D \tag{55}$$

where $D = D_n + \sum_{i=1}^{n}\left(\frac{\sigma}{2}\boldsymbol{\theta}_n^T\boldsymbol{\theta}_n + \frac{\bar{\sigma}_n}{3}l_n^3\right) + \frac{1}{2}\bar{\mathrm{G}}^2$.

Denote $\flat = \min\{2c_i b_{\min}, (2\sigma-1)\eta, 3r\bar{\sigma}_i, i = 1, \cdots, n\}$ with $b_{\min} = \min\{b_i, i = 1, \cdots, n\}$, $\ell = \frac{n}{4\xi} + \frac{1}{2}\sum_{i=1}^{n}(\bar{\varepsilon}_i)^2 + \sum_{i=1}^{n}\left(\frac{\sigma}{2}\boldsymbol{\theta}_i{}^T\boldsymbol{\theta}_i + \frac{\bar{\sigma}_i}{3}l_i^3\right) + \frac{1}{2}\bar{\mathrm{G}}^2$. Then, (55) can be rewritten as:

$$\dot{V} \leqslant -\flat V + \ell \tag{56}$$

Then, (56) can be rewritten as

$$V(t) \leqslant -V(0)e^{-\flat t} + \frac{\ell}{\flat} \tag{57}$$

Based on (56) and (57), we can conclude that all signals, $\boldsymbol{x}_i^f$, $\hat{\boldsymbol{\theta}}_{i-1}$, $\boldsymbol{y}_d^{(i)}$, $\hat{\boldsymbol{l}}_i$ and are ultimately uniformly bounded.

Furthermore, we can also obtain

$$|y(t) - y_d(t)| \leqslant \sqrt{2V(0)}e^{-\frac{\flat}{2}t} + \sqrt{\frac{2\ell}{\flat}} \tag{58}$$

According to the expressions of $\flat$ and ℓ, $\sqrt{2\ell/\flat}$ can be arbitrarily small by increasing b_i, r, η and decreasing ξ. That is to say, the tracking error $|y(t) - y_d(t)|$ can be arbitrarily small by choosing appropriate controller parameters.

Simulation results

The following three simulation examples are given to validate the effectiveness and applicability of the MTN-based control scheme proposed in this paper.

Example 1 (Numerical example): Consider the following second-order nonlinear system with actuator saturation and sensor failure, described as follows

$$\begin{cases} \dot{x}_1 = x_2 - 0.5x_1^2 + \Delta_1(t) \\ \dot{x}_2 = u(v) + x_1x_2^2 + \Delta_2(t) \\ y = x_1 \end{cases} \tag{59}$$

with the initial state is $[x_1(0), x_2(0)]^T = [0, 0]^T$. The tracking signal is set to $y_d = 0.6sint$ and the actuator saturation of the system is set as $u(v) = \begin{cases} 150\text{sign}(v), & |v| \geqslant 150 \\ v & , |v| < 150 \end{cases}$.

According to Theorem 1, the control structure of the system (59) can be designed as

$$\begin{cases} \alpha_1 = -c_1\tilde{z}_1 - \hat{\boldsymbol{\theta}}_1^T\varphi_1(\boldsymbol{Z}_1) \\ v = -\frac{1}{}\left(c_2\tilde{z}_2 + \hat{\boldsymbol{\theta}}_2^T\varphi_2(\boldsymbol{Z}_2)\right) \end{cases} \tag{60}$$

The adaptive laws are designed as

$$\begin{cases} \dot{\hat{\boldsymbol{\theta}}}_i = \tilde{z}_i\varphi_i(\boldsymbol{Z}_i) - \sigma\hat{\boldsymbol{\theta}}_i \\ \dot{\hat{l}}_i = \begin{cases} r\left[\xi c_i^2\tilde{z}_i^2 + c_i + \frac{1}{2}\right]\left(x_i^f\right)^2 - r\bar{\sigma}_i\hat{l}_i, m_i > 0 \\ 0, m_i \leqslant 0 \end{cases} \\ i = 1, 2 \end{cases} \tag{61}$$

In simulation, the controller parameters are selected as $u_m = 150$, $c_1 = 100$, $c_2 = 80$, $\xi = 0.01$, $r = 20$, $\sigma = 2$, $\bar{\sigma}_1 = 12$, $\bar{\sigma}_2 = 4800$, $\underline{g} = 0.15$, $\bar{g} = 1$, $\rho = 0.7$, $\eta = 20$.

The simulation results are shown in Figures 2 to 6. It can be clearly seen that when the sensor fails, the tracking performance of the system can be well ensured. Figure 3 shows the trajectories of u and v. Figure 4 shows the trajectories of adaptive laws $\hat{l}_1$ and $\hat{l}_2$ in the case of fault. It is clear that the adaptive parameter $\hat{l}_i, i = 1, 2$ increases rapidly to mitigate the performance loss when the sensor fails, and the transient stimuli from external input signals prevent the adaptive parameters from converging to their values. Figures 5 and 6 show the trajectories of tracking error and the state x_2, respectively. The simulation results show that all the signals of the system are bounded and the tracking errors are controlled in a small neighbor near the origin and within the set constraints, which demonstrates the effectiveness and rationality of the control strategy.

Example 2 (Practical example): In order to further verify the feasibility of the proposed approach, consider a class of mass-spring-damper system with actuator saturation, according to Johansson et al.,[60] its system can be described as follows

$$\begin{cases} \dot{x}_1 = x_2 \\ \dot{x}_2 = \frac{1}{m}u(v) - \frac{b_1}{m}x_1 - \frac{{b_1}^2}{b_3}mx_1^3 - \frac{b_2}{m}x_2 + d \\ y = x_1 \end{cases} \tag{62}$$

where $m = 1/4$ t and the actuator saturation satisfies $u(v) = \begin{cases} 150\text{sign}(v), & |v| \geqslant 150 \\ v & , |v| < 150 \end{cases}$.

According to Theorem 1, the control structure of the system (62) can be described as (60) and (61).

In the simulation, the parameters of system (62) are set as $b_1 = 1/4$, $b_2 = -1/4$, $b_3 = 1/2$ and $d = 0.5$ $\sin t$. The sensor faults are given as $x_i^f = 0.7x_i, \forall t > T_f$.

The initial state of the system is $[x_1(0), x_2(0)]^T = [0, 0]^T$, the tracking signal is set to $y = 0.6sint$ and the controller parameters in the proposed scheme are chosen as $u_m = 150, c_1 = 76,\ c_2 = 64, \xi_1 = \xi_2 = 0.01, r = 80, \sigma = 2, \bar{\sigma}_1 = 14, \bar{\sigma}_2 = 4000, \underline{g} = 0.15, \bar{g} = 1, \eta = 20$.

The simulation results are shown in Figures 7 to 10, which further verify the effectiveness of the proposed adaptive compensation controller.

Example 3 (Comparative study): In order to highlight the effectiveness and superiority of the proposed method, the following three simulation studies are provided.

Case 1: For system (59), the loss of effectiveness failure ρ select as $\rho = 0.6, 0.7, 0.8, 0.9$ respectively. At the same conditions, the simulation results are shown in Figure 11. From 11, it can be seen that the satisfying control performance can be achieved for different values of ρ.

Case 2: To illustrate the influence of design parameters, we selected parameter c_i as the reference object for the

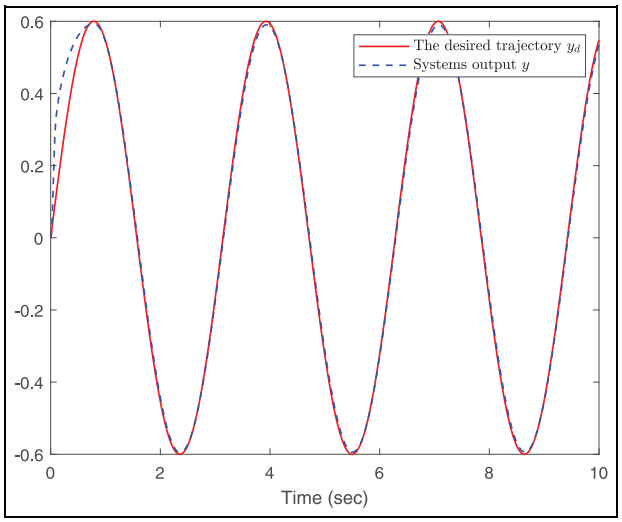

Figure 2. The trajectorie of y and y_d of system (59).

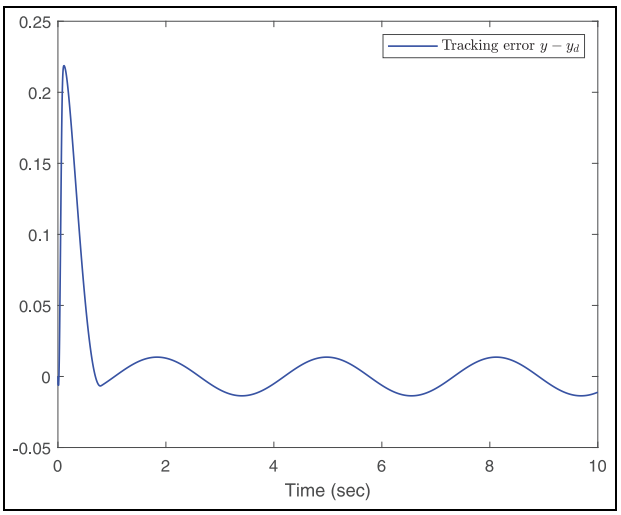

Figure 5. Trajectory of tracking error $y - y_d$ of system (59).

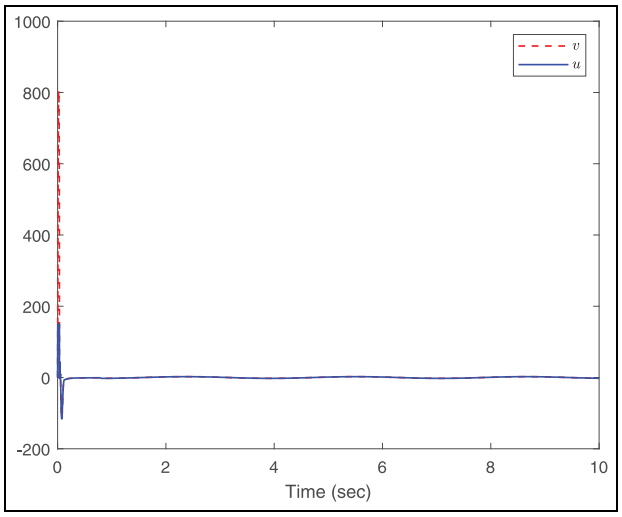

Figure 3. The trajectories of u and v of system (59).

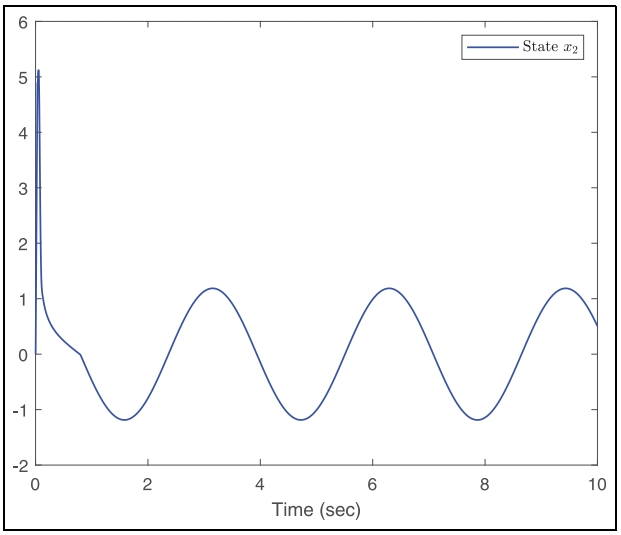

Figure 6. The trajectory of state x_2 of system (59).

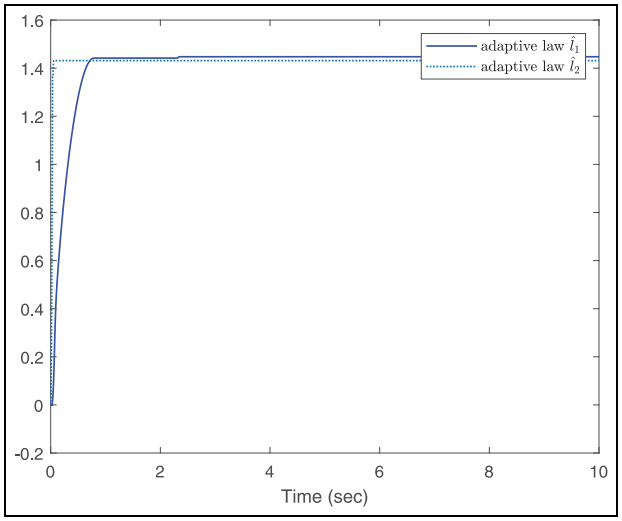

Figure 4. The adaptive laws $\hat{l}_1$ and $\hat{l}_2$ of system (59).

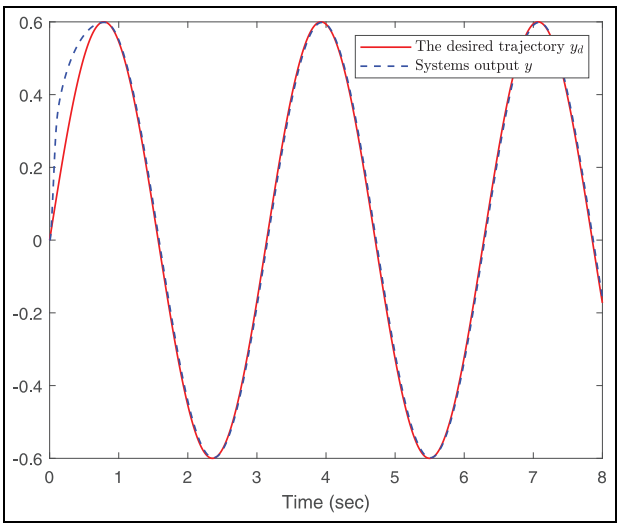

Figure 7. The trajectories of y and y_d of system (62).

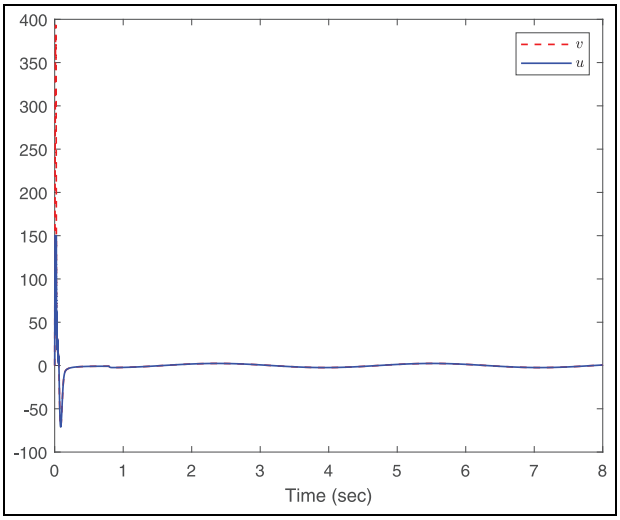

Figure 8. The trajectories of u and v of system (62).

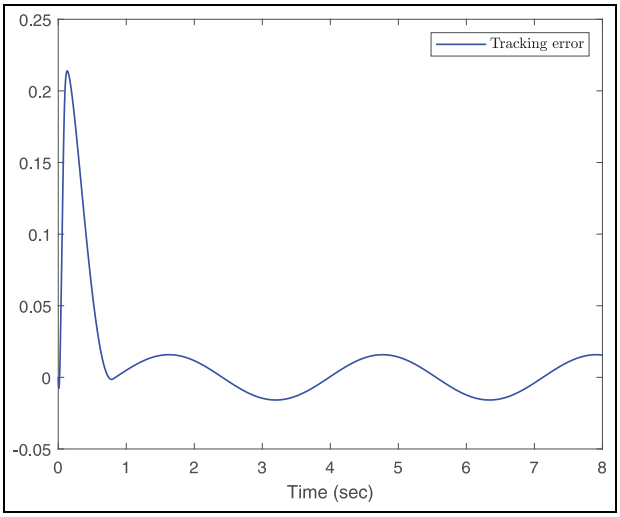

Figure 10. The trajectory of tracking error $y - y_d$ of system (62).

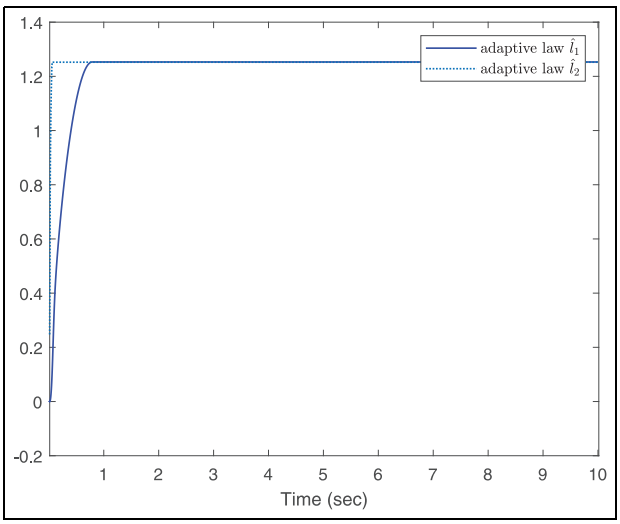

Figure 9. The adaptive laws $\hat{l}_1, \hat{l}_2$ of system (62).

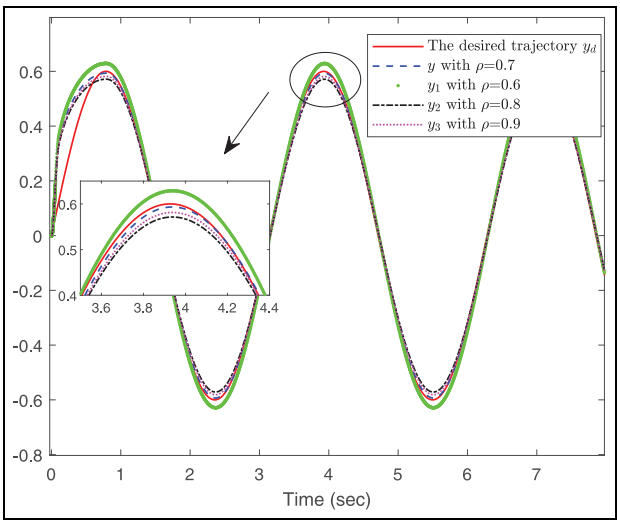

Figure 11. The trajectories of y_i and y_d of system (59).

comparative experiment for system (62). Under the condition that other parameters remain unchanged, c_i is set to $c_i = 60$ and $c_i = 90$, respectively. The simulation results are presented in Figure 12. From Figures 7 and 12, we can see that the tracking performance is best when $c_1 = 76$ and $c_2 = 64$. Therefore, we can conclude that the choice of design parameters does indeed affect tracking performance. As a result, careful selection is required in practical control applications.

Case 3: A comparative experiment was conducted between the adaptive MTN and the RBF neural network (RBFNN) control methods, utilizing system (62) as the basis for comparison. The simulation results are shown in Figure 13. From Figure 13, it can be seen that both methods achieve similarly satisfactory outcomes in this case. However, it should be emphasized that the MTN-based method proposed in this paper has a lower computational burden.

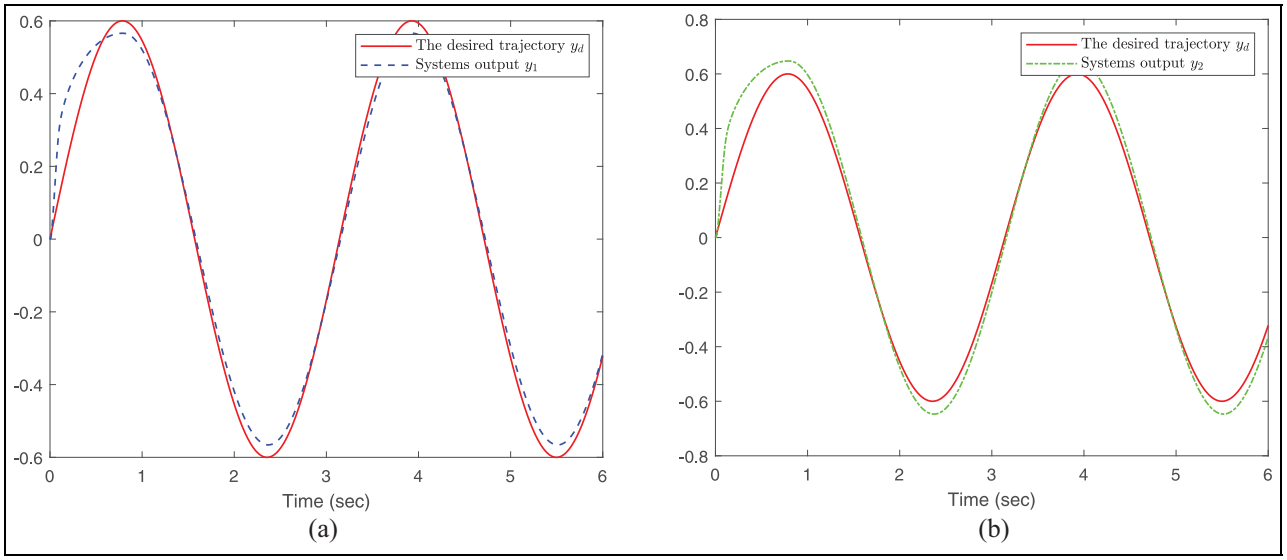

Figure 12. The tracking effect under $c_i = 90$ and $c_i = 60$ of system (62): (a) tracking effect under $c_1 = c_2 = 90$ and (b) tracking effect under $c_1 = c_2 = 60$.

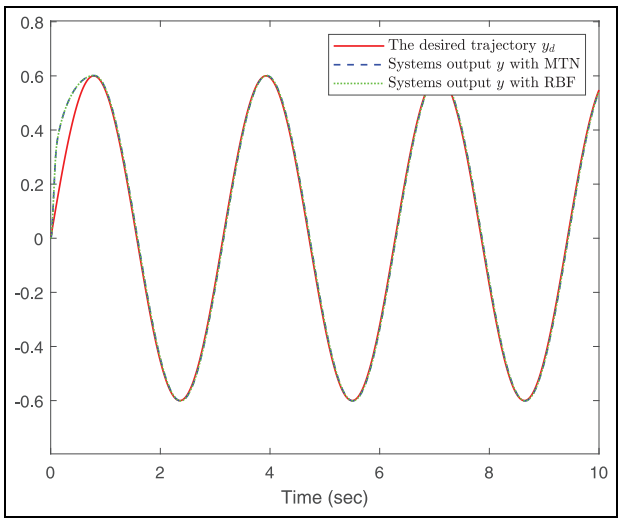

Figure 13. The tracking effect under MTN and RBF of system (62).

Conclusion

This paper investigates the adaptive tracking control problem for a class of uncertain nonlinear systems with actuator saturation and multi-sensor faults. Multiple adaptive signal compensation mechanisms are used to eliminate the adverse effects of sensor faults. Compared with previous results, not only the effect of multi-sensor faults on the system but also the actuator saturation is considered, and the designed controller is able to quickly capture the effective conditions from the fault information to achieve the tracking effect. All signals of the closed-loop system are guaranteed to be bounded by MTN approximation of the unknown function and combined with Lyapunov stability theory. Simulation results demonstrate the effectiveness of the proposed control method.

Declaration of conflicting interests

The author(s) declared no potential conflicts of interest with respect to the research, authorship, and/or publication of this article.

Funding

The author(s) disclosed receipt of the following financial support for the research, authorship, and/or publication of this article: This work was supported by the Shandong Provincial Natural Science Foundation, China (No. ZR2020QF055).

ORCID iD

Yu-Qun Han https://orcid.org/0000-0002-9055-2954

Data availability

Data sharing is not applicable to this article as no new data were created or analyzed in this study.

References

1. Li YM, Tong SC and Li TS. Composite adaptive fuzzy output feedback control design for uncertain nonlinear strict-feedback systems with input saturation. *IEEE Trans Cybern* 2015; 45(10): 2299–2308.
2. Ma JJ, Zheng ZQ and Li P. Adaptive dynamic surface control of a class of nonlinear systems with unknown direction control gains and input saturation. *IEEE Trans Cybern* 2015; 45(4): 728–741.
3. Ji RH, Ge SZS and Li DY. Saturation-tolerant prescribed control for nonlinear systems with unknown control directions and external disturbances. *IEEE Trans Cybern* 2024; 54(2): 877–889.
4. Zhang LL and Yang GH. Adaptive fuzzy fault compensation tracking control for uncertain nonlinear systems with multiple sensor faults. *Fuzzy Sets Syst* 2020; 392: 46–59.

5. Wu F, Lin ZL and Zheng Q. Output feedback stabilization of linear systems with actuator saturation. *IEEE Trans Automat Contr* 2007; 52(1): 122–128.
6. Li Y, Tong S and Li T. Adaptive fuzzy output-feedback control for output constrained nonlinear systems in the presence of input saturation. *Fuzzy Sets Syst* 2014; 248: 138–155.
7. Han YQ and Sun JJ. Adaptive finite-time control for a class of stochastic nonlinear systems with input saturation constraints: a new approach based on multidimensional Taylor network. *Int J Robust Nonlinear Control* 2024; 34(8): 5329–5345.
8. Li HY, Wang JH and Shi P. Output-feedback based sliding mode control for fuzzy systems with actuator saturation. *IEEE Trans Fuzzy Syst* 2016; 24(6): 1282–1293.
9. Lu L and Lin ZL. Design of switched linear systems in the presence of actuator saturation. *IEEE Trans Automat Contr* 2008; 53(6): 1536–1542.
10. Lin D, Wang XY and Yao Y. Fuzzy neural adaptive tracking control of unknown chaotic systems with input saturation. *Nonlinear Dyn* 2012; 67: 2889–2897.
11. Chen M, Ge SZ and Ren BB. Adaptive tracking control of uncertain MIMO nonlinear systems with input constraints. *Automatica* 2011; 47(3): 452–465.
12. Guo XG, Zhao JJ, Li HJ, et al. Novel auxiliary saturation compensation design for neuroadaptive NTSM tracking control of high speed trains with actuator saturation. *J Franklin Inst* 2020; 357(3): 1582–1602.
13. Zhai D, An LW, Dong JX, et al. Output feedback adaptive sensor failure compensation for a class of parametric strict feedback systems. *Automatica* 2018; 97: 48–57.
14. Wang HQ, Chen B, Liu XP, et al. Adaptive neural tracking control for stochastic nonlinear strict-feedback systems with unknown input saturation. *Inf Sci* 2014; 269: 300–315.
15. Wen CY, Zhou J, Liu ZT, et al. Robust adaptive control of uncertain nonlinear systems in the presence of input saturation and external disturbance. *IEEE Trans Automat Contr* 2011; 56(7): 1672–1678.
16. Bey O and Chemachema M. Decentralized event-triggered output feedback adaptive neural network control for a class of MIMO uncertain strict-feedback nonlinear systems with input saturation. *Int J Adapt Control Signal Process* 2024; 38(4): 1420–1441.
17. Bey O and Chemachema M. Finite-time event-triggered output-feedback adaptive decentralized echo-state network fault-tolerant control for interconnected pure-feedback nonlinear systems with input saturation and external disturbances: a fuzzy control-error approach. *Inf Sci* 2024; 669: 120557.
18. Bey O and Chemachema M. Control-error-based output-feedback adaptive decentralized neural network controller for interconnected uncertain strict-feedback nonlinear systems with input saturation. *Trans Inst Meas Control* 2024; 46(8): 1529–1541.
19. Gao SG, Dong HR, Chen Y, et al. Approximation-based robust adaptive automatic train control: an approach for actuator saturation. *IEEE trans Intell Transp Syst* 2013; 14(4): 1733–1742.
20. Bounemeur A, Chemachema M and Essounbouli N. Indirect adaptive fuzzy fault-tolerant tracking control for mimo nonlinear systems with actuator and sensor failures. *ISA Trans* 2018; 79: 45–61.
21. Carneiro DDS, Faria FA, Silva LJR, et al. Robust sampled-observer-based switching law for uncertain switched affine systems subject to sensor faults with an application to a bidirectional buck-boost DC-DC converter. *IEEE Access* 2024; 12: 87967–87980.
22. Lin GH, Li HY, Ma H, et al. Human-in-the-loop consensus control for nonlinear multi-agent systems with actuator faults. *IEEE/CAA J Autom Sin* 2022; 9(1): 111–122.
23. Zhai D, An LW, Li XJ, et al. Adaptive fault-tolerant control for nonlinear systems with multiple sensor faults and unknown control directions. *IEEE Trans Neural Netw Learn Syst* 2018; 29(9): 4436–4446.
24. Liu H, Pan YP, Cao JD, et al. Adaptive neural network backstepping control of fractional-order nonlinear systems with actuator faults. *IEEE Trans Neural Netw Learn Syst* 2020; 31(12): 5166–5177.
25. Wang HQ, Bai W, Zhao XD, et al. Finite-time-prescribed performance-based adaptive fuzzy control for strict-feedback nonlinear systems with dynamic uncertainty and actuator faults. *IEEE Trans Cybern* 2022; 52(7): 6959–6971.
26. Meng YH, Zhang Y, Ye H, et al. Trajectory tracking control for unmanned amphibious surface vehicles with actuator faults. *Appl Ocean Res* 2024; 152: 104182–104182.
27. You FQ, Li H, Zhang YW, et al. A novel sensor fault diagnosis approach for time-varying delay systems with non-linear uncertainty. *Trans Inst Meas Control* 2017; 39(7): 1114–1120.
28. Wang X and Tan CP. Output feedback active fault tolerant control for a 3-dof laboratory helicopter with sensor fault. *IEEE Trans Autom Sci Eng* 2024; 21(3): 2689–2700.
29. Wang JH, Liu JR, Li YH, et al. Prescribed time fuzzy adaptive consensus control for multiagent systems with dead-zone input and sensor faults. *IEEE Trans Autom Sci Eng* 2024; 21(3): 4016–4027.
30. Zhang Q and Zhang XD. Distributed sensor fault diagnosis in a class of interconnected nonlinear uncertain systems. *Annu Rev Control* 2013; 37(1): 170–179.
31. Zhang LL and Yang GH. Observer-based fuzzy adaptive sensor fault compensation for uncertain nonlinear strict-feedback systems. *IEEE Trans Fuzzy Syst* 2018; 26(4): 2301–2310.
32. Guo XJ, Wang J and Sun WC. Nonlinear adaptive fault-tolerant control for full-car active suspension with velocity measurement errors and full-state constraints. *J Franklin Inst* 2024; 361(10): 106845.
33. Yue S, Chuang G, Bing WL, et al. Fuzzy observer-based command filtered tracking control for uncertain strict-feedback nonlinear systems with sensor faults and event-triggered technology. *Nonlinear Dyn* 2023; 111(9): 8329–8345.
34. Xiong SS and Hou ZS. Data-driven formation control for unknown MIMO nonlinear discrete-time multi-agent systems with sensor fault. *IEEE Trans Neural Netw Learn Syst* 2022; 33(12): 7728–7742.
35. Huang XC, Wen CY and Song YD. Adaptive neural control for uncertain constrained pure feedback systems with severe sensor faults: a complexity reduced approach. *Automatica* 2023; 147: 110701.
36. Wang JQ, Fang F, Yi XJ, et al. Dynamic event-triggered fault estimation and sliding mode fault-tolerant control for networked control systems with sensor faults. *App Math Comp Sci* 2021; 389: 125558.

37. Talebi HA, Khorasani K and Tafazoli S. A recurrent neural-network-based sensor and actuator fault detection and isolation for nonlinear systems with application to the satellite's attitude control subsystem. *IEEE Trans Neural Netw* 2009; 20(1): 45–60.
38. Wang H, Lu K, Zheng F, et al. Improved finite-time prescribed performance based adaptive neural control for nonlinear systems with sensor faults. *Neurocomputing* 2023; 560: 126794.
39. Xiong Y, Wu YF and Xiang ZR. Fuzzy adaptive output feedback fault-tolerant control for nonlinear switched large-scale systems with sensor faults. *IEEE Syst J* 2022; 16(3): 3782–3793.
40. He WJ, Zhu SL, Lu LT, et al. A novel network-based adaptive fault-tolerant control of switched nonlinear systems subject to multiple faults under prescribed performance. *ISA Trans* 2024; 145: 78–86.
41. Li N, Han YQ, He WJ, et al. A novel network-based controller design for a class of stochastic nonlinear systems with multiple faults and full state constraints. *Int J Control* 2024; 97(4): 651–661.
42. Yan HS and Li CL. MTN-based recursive *d*-step-ahead predictive control of MIMO nonlinear systems with unknown input time-delay in industrial process. *Assem Autom* 2022; 42(4): 474–489.
43. He WJ, Zhu SL, Lu LT, et al. Adaptive multi-switching-based global tracking control for switched nonlinear systems with prescribed performance. *IEEE Trans Autom Sci Eng* 2024; 21(3): 3243–3252.
44. Wang MX, Zhu SL, Liu SM, et al. Design of adaptive finite-time fault-tolerant controller for stochastic nonlinear systems with multiple faults. *IEEE Trans Autom Sci Eng* 2023; 20(4): 2492–2502.
45. Zhao W, Zhu SL, Zhou YF, et al. Adaptive prescribed performance tracking control for uncertain nonlinear systems with unknown backlash-like hysteresis. *Proc IMechE, Part I: J Systems and Control Engineering* 2024; 238(7): 1206–1218.
46. He X and Jia Fl. Active fault-tolerant control for nonlinear systems with nonlogarithmic sensor resolution. *IEEE Trans Instrum Meas* 2024; 73: 1–11.
47. Zhang ZY, Yang XS, Lam HK, et al. Event-triggered control for switched systems with sensor faults via adaptive fuzzy observer. *Math Comput Simul* 2024; 221: 244–259.
48. Li DP, Han HG and Qiao JF. Fuzzy-approximation adaptive fault tolerant control for nonlinear constraint systems with actuator and sensor faults. *IEEE Trans Fuzzy Syst* 2024; 32(5): 2614–2624.
49. Gao YF, Sun XM, Wen CY, et al. Adaptive tracking control for a class of stochastic uncertain nonlinear systems with input saturation. *IEEE Trans Automat Contr* 2017; 62(5): 2498–2504.
50. Min HF, Xu SY, Zhang BY, et al. Output-feedback control for stochastic nonlinear systems subject to input saturation and time-varying delay. *IEEE Trans Automat Contr* 2019; 64(1): 359–364.
51. Liu PD, Zhang HY, Ming ZY, et al. Dynamic event-triggered safe control for nonlinear game systems with asymmetric input saturation. *IEEE Trans Cybern* 2024; 54(9): 5115–5126.
52. Zhang HY, Zhao XD, Wang HQ, et al. Adaptive tracking control for output-constrained switched MIMO pure-feedback nonlinear systems with input saturation. *J Syst Sci Complex* 2023; 36(3): 960–984.
53. Wu ZW, Zhang TP, Xia XN, et al. Finite-time adaptive neural command filtered control for non-strict feedback uncertain multi-agent systems including prescribed performance and input nonlinearities. *Appl Math Comput* 2022; 421: 126953.
54. Yang B, Xiao WB, Yin H, et al. Adaptive neural control for multiagent systems with asymmetric time-varying state constraints and input saturation. *Int J Robust Nonlinear Control* 2020; 30(12): 4764–4778.
55. Mu YF, Zhang HG, Xi RP, et al. Fault-tolerant control of nonlinear systems with actuator and sensor faults based on T–S fuzzy model and fuzzy observer. *IEEE Trans Syst Man Cybern Syst* 2022; 52(9): 5795–5804.
56. Han YQ and Sun JJ. Adaptive finite-time control for a class of stochastic nonlinear systems with input saturation constraints: a new approach based on multi-dimensional Taylor network. *Int J Robust Nonlinear Control* 2024; 34(8): 5329–5345.
57. Wang DM, Han YQ, Lu LT, et al. Dynamic event-triggered adaptive tracking control for stochastic nonlinear systems with deferred time-varying constraints. *Chaos Solitons Fractals* 2024; 182: 114814.
58. Lu LT, Zhu SL, Wang DM, et al. Predefined-time adaptive consensus control for nonlinear multi-agent systems with input quantization and actuator faults. *Nonlinear Dyn* 2024; 112(16): 1–20.
59. Zhang LL and Yang GH. Adaptive fuzzy fault compensation tracking control for uncertain nonlinear systems with multiple sensor faults. *Fuzzy Sets Syst* 2020; 392: 46–59.
60. Johansson KH, Egerstedt M, Lygeros J, et al. On the regularization of Zeno hybrid automata. *Syst Control Lett* 1999; 38(3): 141–150.